Environmental Technology & Innovation 36 (2024) 103871

Contents lists available at ScienceDirect

Environmental Technology & Innovation

journal homepage: www.elsevier.com/locate/eti

Efficacious enrichment of butyrate-oxidizing exoelectrogens upgrades energy recovery in relevant bioelectrochemical systems

Ahmed Elreedy [a,1], Daniel Härrer [b,1], Rowayda Ali [c], Andrea Hille-Reichel [c], Johannes Gescher [a,b,*]

[a] Institute of Technical Microbiology, Hamburg University of Technology, Hamburg 21073, Germany
[b] Institute for Applied Biosciences, Department of Applied Biology, Karlsruhe Institute of Technology, Karlsruhe 76131, Germany
[c] Engler-Bunte-Institut, Water Chemistry and Water Technology, Karlsruhe Institute of Technology, Engler-Bunte-Ring 9a, Karlsruhe 76131, Germany

ARTICLE INFO

Keywords:
Microbial electrolysis cell
Anodic biofilm
Coulombic efficiency
Geobacter
Butyrate kinase
Hydrolysate treatment

ABSTRACT

Energy recovery via bioelectrochemical systems (BESs) while treating organic wastes has proven to be a promising technology. Organic waste hydrolysates are appealing feedstocks for BESs due to their richness in short-chain fatty acids rather than complex organics. However, butyrate, among the abundant acids in hydrolysates, has been found to particularly hinder the efficiency of BESs. The lack of efficient anodic butyrate-oxidizers appears to be critical; therefore, this study targeted the enrichment of an anodic community to enhance butyrate oxidation efficiency in BESs. We initially tested three different inoculum sources using butyrate as the sole electron donor. Then, through successive transfers of a bioanode piece to fresh anodes, significant improvement in coulombic efficiency (CE) from 9.4 % to 78.6 % was achieved over six transfers. The enriched bioanode was dominated by the bacterial genera *Geobacter* (72 %) and *Sporomusa* (16 %), which correlated positively with CE development over transfers. The metagenomic/transcriptomic analyses confirmed the key role of *Geobacter* in the anodic oxidation of butyrate, while *Sporomusa* likely displayed a syntrophic interaction, assimilating acetate from CO_2 and excess H_2. The enriched culture was further bioaugmented with *Geobacter sulfurreducens* and tested with real butyrate-containing hydrolysate, in which CE and maximum current density of 86.9 % and ~3.5 A/m^2 were achieved, respectively. Overall, the enriched butyrate-oxidizing culture, bioaugmented with *G. sulfurreducens*, proves efficient for BESs treating butyrate-rich waste-streams.

1. Introduction

The need to overcome a future shortage of resources and energy gives rise to the development of innovative and practical technologies for generating low-emission energy from biogenic waste streams. This has raised increasing interest in bioelectrochemical systems (BESs), where energy recovery can be achieved in parallel to wastewater treatment, either in the form of electricity via microbial fuel cells (MFCs) or as hydrogen via microbial electrolysis cells (MECs). Technologies relying on the anaerobic oxidation of organic loads can serve as

* Corresponding author at: Institute of Technical Microbiology, Hamburg University of Technology, Hamburg 21073, Germany.
E-mail address: johannes.gescher@tuhh.de (J. Gescher).
[1] The authors contributed equally.

https://doi.org/10.1016/j.eti.2024.103871
Received 14 March 2024; Received in revised form 18 October 2024; Accepted 25 October 2024
Available online 28 October 2024

energy-efficient alternatives to conventional wastewater treatment plants. In these plants, the most energy-consuming process for pollutant elimination is aeration, with no energy gained in return (Madjarov et al., 2016). The MEC applications gain special attention since hydrogen is considered an important sustainable energy carrier of the future. MEC has also been combined with anaerobic digestion (AD) process for the aim of improving methane productivity via balancing the electron fluxes. In BESs, anode-respiring microorganisms catalyze the oxidation of organic compounds on the electrode surface. Such microorganisms conduct extracellular electron transfer (EET) as part of their natural anaerobic metabolism (Logan and Regan, 2006; Lovley, 2006). The microbial electron transfer chains transport electrons from low-potential electron donors (e.g., organic acids) to acceptors with a more positive redox potential (e.g., poised anodes) through a series of redox reactions, resulting in a flow of electrons, i.e., electrical current (Brunner et al., 2019).

With regards to the responsible biocatalysts in this process, *Geobacter sulfurreducens* and *Shewanella oneidensis* are the most extensively studied exoelectrogens (Jing et al., 2022; Klein et al., 2023). However, the fact that they are known to oxidize only certain organic acids (mostly acetate and lactate) has limited their complying with various industrial applications. Meanwhile, syntrophic interactions with other organisms are likely necessary when dealing with complex organics, e.g., cellulose, hemicellulose, fats, proteins, sugars, alcohols, and longer-chain fatty acids (e.g., butyrate, valerate, and oleate) (Brunner et al., 2019; Kokko et al., 2018). For this, using mixed culture as inoculum is suitable; however, the complexity of substrates and induced microbial diversity contribute unfavorably to the emergence of side reactions (Logan et al., 2015). Such reactions reduce the current production and coulombic efficiency (CE) in BESs, as widely reported to date (Choi et al., 2023; He et al., 2016; Kokko et al., 2018; Miceli et al., 2014; Pandey et al., 2016; Rossi et al., 2022). To address this limitation, on the one hand, careful substrate characterization is needed to define potentially inhibiting components; on the other hand, the proper selection and/or enrichment of inoculum is crucial to guarantee optimized performance. For instance, the hydrolysate from dark fermentation processes, primarily composed of short-chain organic acids (e.g., acetate, propionate, butyrate, and valerate), holds promise as an appealing substrate for BESs. Nonetheless, excessive levels of certain acids, such as butyrate, which is abundant in various hydrolysates, could substantially limit the potential for energy recovery (Choi et al., 2023; Lin et al., 2019; Zhang et al., 2022). Concerning this, we could previously prove the significant hindering effect of butyrate ($\geq$ 10 mM) on *G. sulfurreducens* (Härrer et al., 2022). In that study, we also demonstrated that *G. sulfurreducens* has a high potential to oxidize acetate and generate high current density when exposed to a low concentration of hydrolysate; therefore, it would be mutually beneficial for the overall BESs efficiency if efficient bioanodic oxidation of butyrate could be integrated, since butyrate is often one of the most abundant acids present in such fermentation broths.

When looking in the literature for BESs operated with butyrate as the sole electron donor, most of them belonged to the MFC-mode, with low reported CEs (5–56 %) (Freguia et al., 2010; Liu et al., 2005; Min and Logan, 2004; Torres et al., 2007; Yu et al., 2015; Zhang et al., 2022, 2011). Higher CE of up to 72 % was only reported when using low butyrate concentrations of 4–7 mM (Freguia et al., 2010; Yang et al., 2015). Hence, a crucial key to improving the stability and performance of relevant BESs is obtaining an efficient and robust biocatalyst. Ways to achieve this may start with investigating various environmental samples to find the appropriate inoculum. Second, employing an efficient enrichment strategy have proven to reduce startup periods and/or boost the productivity of BESs, such as using inoculum collected from the planktonic phase of a running BES or preconditioned inoculum harvested from a biofilm (Baudler et al., 2014; Blanchet et al., 2015; Riedl et al., 2017; Zhang et al., 2013). Another reported strategy considered combining pure and mixed cultures, as inoculum, which allows for the integration of multiple electron transfer mechanisms (Guang et al., 2020). This not only addresses fluctuations in populations resulting from the process but also facilitates the transfer of respiratory electrons, which are not exoelectrogenically generated, to the electrode. The beneficial synergy arising from this approach can improve current density, CEs, and achieve long-term process stability.

Given the abovementioned challenges/opportunities, we here aimed at enriching an anodic butyrate-oxidizing community to serve as an efficient biocatalyst within BESs dealing with butyrate-rich effluents. For this, inocula sourced from different environmental samples were initially tested with butyrate as sole electron donor. Then, an adopted enrichment strategy based on isolating the effective anode-respiring bacteria was investigated, seeking for maximum achievable CE. The evolving composition of the anodic community was carefully studied, along with the identification of responsible microbes. Moreover, metagenomic/transcriptomic analysis was conducted to elucidate the major metabolic pathways involved. Potential bioaugmentation of such anodic culture with the model exoelectrogen *G. sulfurreducens* was also examined. Eventually, the efficiency of enriched culture was assessed in a BES fed with real hydrolysate. The insights derived from this approach will help in optimizing the industrial applicability of BESs for simultaneous energy recovery and wastewater treatment.

2. Materials and methods

2.1. Inocula and enrichment medium

Inocula from three different sources were initially tested separately in this study, i.e., cow manure (30–40 cm-depth), hydrolysis sludge (from a running acid-fermenter that uses vegan dog food as substrate (Ali et al., 2021)), and anoxic sediment (20–40 cm-depth; from nearby the Nagold Dam, Freudenstadt, Germany). A modified *G. sulfurreducens* medium (DMSZ, media 141) with 10 mM-butyrate (instead of acetate) as the sole electron donor was used for enrichment in BESs. Sterilization of medium was performed by autoclaving, whereas heat-sensitive components (e.g., vitamins) were sterilized using a 0.2 μm membrane filter. In addition, the hydrolysate used, for final validation using a real complex feed, was collected from a running 12 L-fermenter (Ali et al., 2021). The hydrolysate was then centrifuged two times, step-filtered (1 and then 0.45 μm), sterile-filtered (0.2 μm), and kept at 4°C until being used in the here described experiment. The organic and inorganic constituents of the hydrolysate were analyzed as presented earlier (Härrer et al., 2022). Due to the high concentrations of organic acids in such hydrolysate, i.e., 65 mM-butyrate, 122 mM-acetate, and 60

mM-propionate, 50 %-diluted feed was used for the desired experiment.

2.2. BESs setup and experimental design

A two chambers and three-electrode cylindrical-BES (C-BES) with a working volume of 250 mL was used, consisting of graphite-felt (36 cm^2; GFD 2.5, SGL Carbon, Germany) as anode, Ag/AgCl reference electrode (+199 mV vs normal hydrogen electrode [NHE]; SE10, Xylem Analytics, Germany), and platinum-mesh (104 mesh/cm^2, Chempur, Germany) as cathode (Fig. S1a). An anodic potential of 0 mV vs NHE (equivalent to −199 mV vs Ag/AgCl) was set for the chronoamperometric measurement using an EmStat3 potentiostat (PalmSens BV, Randhoev, Netherlands). The BESs were placed in a 30°C incubator, stirred with magnetic stirrers, and the headspace was continuously flushed with N_2/CO_2 (80/20 %). Unless otherwise mentioned, all experimental runs were performed in a batch-mode. The aimed enrichment strategy in this study started with testing inocula from three different sources. The three selected inocula were added to three C-BESs with an initial concentration of 1 % (v/v). Second, the enrichment proceeded with the inoculum that achieved the highest efficiency. For the enrichment, selective isolation of the exoelectroactive community by successive transfers was employed as studied previously by Riedl et al. (2017), where an exclusion of microorganisms with potential side reactions can be attained. Meanwhile, first, a series of experiments were conducted to probe the best transfer strategy. Afterwards, such transferring was repeated for the aim of maximizing the CE. This ended up with six generations of selection for butyrate oxidizers, in this study. Transferring the bioanode pieces between BESs was performed in an anaerobic chamber. The transfer of bioanode pieces was performed by cutting a piece (1×3 cm) from a previously enriched anode and then attaching it, via needles, to a fresh anode in a new BES, resulting in a new enrichment generation. Third, the bioaugmentation of the process by adding the model electroactive microorganism *G. sulfurreducens* (OD_{600} of 0.1) was examined, given that release of acetate and potentially H_2 (i.e., suitable substrates for *G. sulfurreducens*) is expected as intermediates during the oxidation of butyrate. *G. sulfurreducens* PCA (DSM No. 12127) was used in this experiment. Eventually, the efficiency of the enriched butyrate-oxidizing community, with highest CE, was tested with real butyrate-rich hydrolysate as anolyte. This experiment was performed using another configuration, namely Flat-plate-BES (FP-BES; Fig. S1b) as previously described (Härrer et al., 2022), where a 2-times higher anodic surface area-to-volume ratio and better flow pattern above the bioanode surface were employed. The recirculation of hydrolysate (as the anolyte) was conducted at a constant flow rate of 20 mL/min. The hydrolysate (50 %-diluted) was then introduced gradually until observing a significant drop in generated current, at which point a switch to a batch-mode is employed.

2.3. Microbial analysis

2.3.1. 16S rDNA amplicon sequencing

Illumina sequencing was used for the phylogenetic and physiological characterization of the butyrate-oxidizing microbial community during the enrichment process. Initially, 16S rDNA amplicon sequencing was performed for samples collected from both the bioanodes and planktonic phases, collected from each enrichment generation. Isolation of genomic 16S rDNA was performed using the DNeasy Power-Biofilm Kit (Qiagen) according to the manufacturer's protocol. The sampling was performed in an anoxic chamber. For this, 2 mL of pelleted planktonic phase as well as a piece of electrode (~1.75 cm^2) were prepared for each sampling point. The planktonic pellet was used directly, while the piece of electrode was divided into smaller pieces before starting the protocol. The concentration and purity of the isolated 16S rDNA was determined using NanoDrop 2000 spectrophotometer (Thermo Fisher Scientific) and stored at −20°C until further use. The forward and reverse primers 341bf (ACACTCTTTCCCTACACGACGCTCTTCCGATCTCCTACGGGNGGCWGCAG) and Uni518r (GACTGGAGTTCAGACGTGTGCTCTTCCGATCTWTTACCGCRGCTGCTGG) were used, respectively. Illumina NextSeq 550 platform and high output Kit V 2.5 (150 cycles) were considered for sequencing, which was performed at the Institute of Biological Interfaces at Karlsruhe Institute of Technology (KIT). The raw data processing of 16S rDNA amplicon sequencing was performed using the CLC genomics workbench (version 12.5, CLC bio, Aarhus, Denmark) using the Microbial Genomic Plugin (version 4.0, Qiagen, Hilden, Germany). The analysis was performed according to a workflow implemented by the manufacturer (OTU Clustering CLC). Here, default settings were used for the first three steps (adapter-trimming, reads-merging, and reads-trimming). The subsequent operational taxonomic unit clustering (OTU-clustering) was performed assuming 97 % relatedness. This involved grouping reads into so-called clusters, where each read had to have a similarity of at least 97 % to every other member of the cluster. The comparison of these clusters with silva database (ver. 128) enabled the phylogenetic assignment of the OTUs. Identification and filtering out of so-called chimeras (artifacts of PCR amplification) was performed in parallel. In the last step, OTU clusters with an abundance of less than 10 reads across all generations were removed. In addition, to show the potential correlations between different bacteria and resulting CE among all samples (based on spearman and p-value of <0.05), network diagrams were also included using Gephi 0.9.2.

2.3.2. Meta-genomic and -transcriptomic analyses

The DNA extraction for the metagenomic analysis was performed similarly as mentioned above only for samples from the 6th generation of enriched butyrate oxidizers. In parallel, at the time of collecting samples, planktonic and anodic samples were mixed with 1 mL of RNA-protect and stored at −80°C until used for the meta-transcriptomic analysis. Isolation of RNA was performed using RNeasy Power-Biofilm Kit (Qiagen) under RNAse free conditions. The concentration and purity of the isolated RNA was checked photometrically. For further quality control of the RNA and to check for DNA residues, PCR was performed. For this purpose, 1 µL of the isolated RNA was mixed with the primers Bacteria_27F (GAGTTTGATCCTGGCTCA) and Bacteria_1525R (AGAAAGGAGGTGATCCAGCC) (Rainey et al., 1994) in a 15 µL Mango-Mix batch. An *E. coli* K12 colony served as positive control and nuclease-free water served as negative control. PCR reactions were then subjected to qualitative gel electrophoresis. If necessary, DNase I digestion was repeated until no DNA could be detected in the RNA samples. The metagenome sequence libraries were generated using the

NEBNext Ultra TM II FS DNA Library and Prep Kit (New England Biolabs, Frankfurt am Main, Germany). The analysis of the meta-genome and -transcriptome datasets presented in this work were performed using the command line-based SqueezeMeta pipeline (Tamames and Puente-Sánchez, 2019). The taxonomic classification of the processed metagenome data was performed by aligning the coding regions with the Diamond database. All raw sequencing data can be accessed through NCBI via SRA accession PRJNA1025973.

2.4. Analytical methods

The organic compounds butyrate, acetate, and propionate were measured by using high-performance liquid chromatography (HPLC; Thermo Fisher Scientific, Germany). The device was equipped with Aminex HPX-87H column (300 × 7.8 mm, Bio-Rad, Munich), UV-detector (at $\lambda = 275$ nm), and Chromeleon 11 software. The applied processing method includes a flow rate of 0.6 mL/min, column temperature of 45°C, and 5 mM H_2SO_4 as mobile phase. Inorganic constituents such as anions and cations were measured using Dionex ICS-1100 (Thermo Fisher Scientific, Waltham, USA). The columns Ion-Pac™ AS9-HC and Ion-Pac™ SCS 1 with 9 mM $NaHCO_3$ and 3 mM CH_3SO_3H as eluents were used for the detection of anions and cations, respectively. The applied processing method, in both cases, includes a flow rate of 0.25 mL/min and column temperature of 30°C. The dissolved organic carbon (DOC) and inorganic carbon (IC) were measured by using TOC analyzer TH600 (Analytic Jena, Jena). Before the abovementioned analyses of samples, they were filtered through 0.2 μm syringe filters. For the calculation of CE, Eq. 1 was used where I (A) is the generated current over time t (sec), F is faraday's constant (96485), b is the number of theoretical moles of electrons released per mole of oxidized compound (i.e., 8 for acetate, 20 for butyrate, and 4 for DOC), and Δ (M) is the reduced concentration of electron donor (e.g., butyrate and acetate) during the time period t.

$$CE(\%) = \frac{\int_0^t Idt}{F \times b \times \text{working volume(L)} \times \quad \Delta \quad (M)} \tag{1}$$

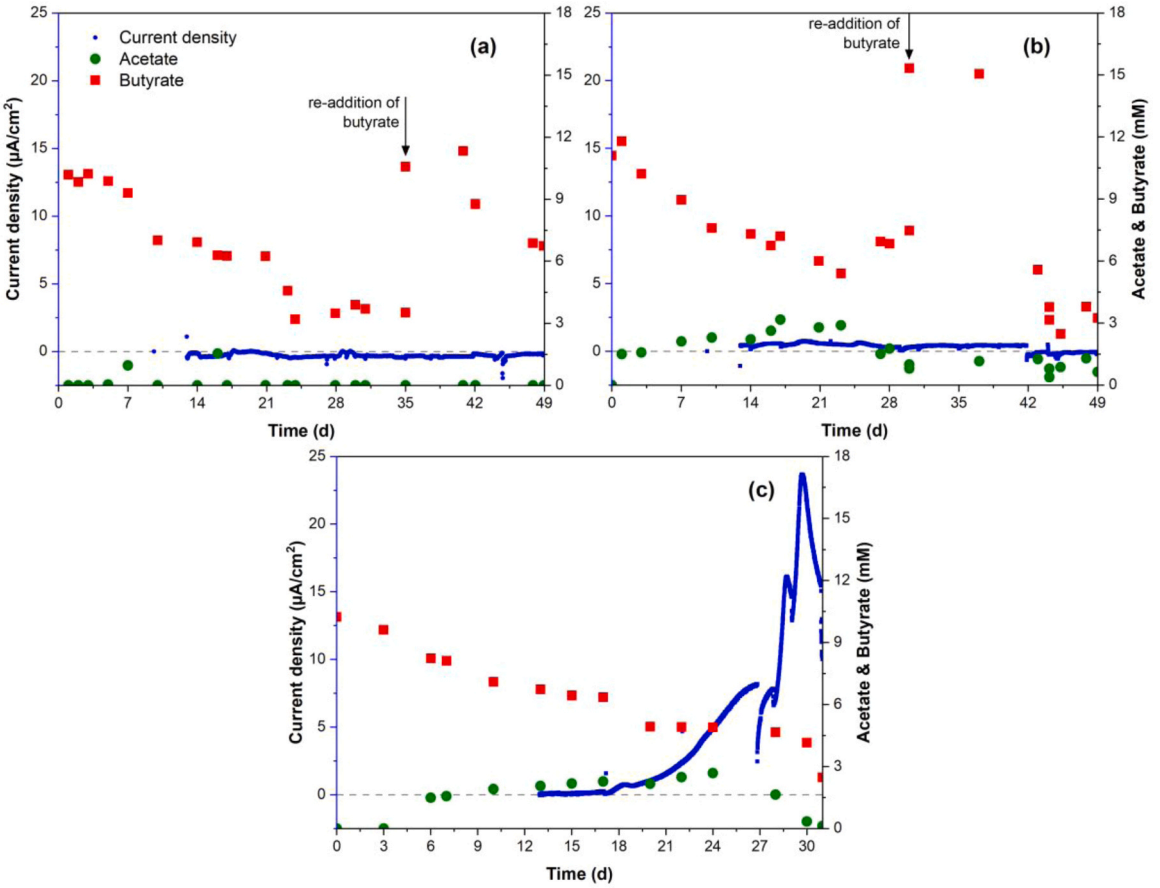

Fig. 1. The time course of current density, acetate, and butyrate in bioelectrochemical systems (BESs) inoculated with cow manure (a), hydrolysis sludge (b), and sediment (c), and fed with butyrate-based medium. Additional butyrate was added when being depleted, as shown. (For interpretation of the references to color in this figure legend, the reader is referred to the web version of this article.).

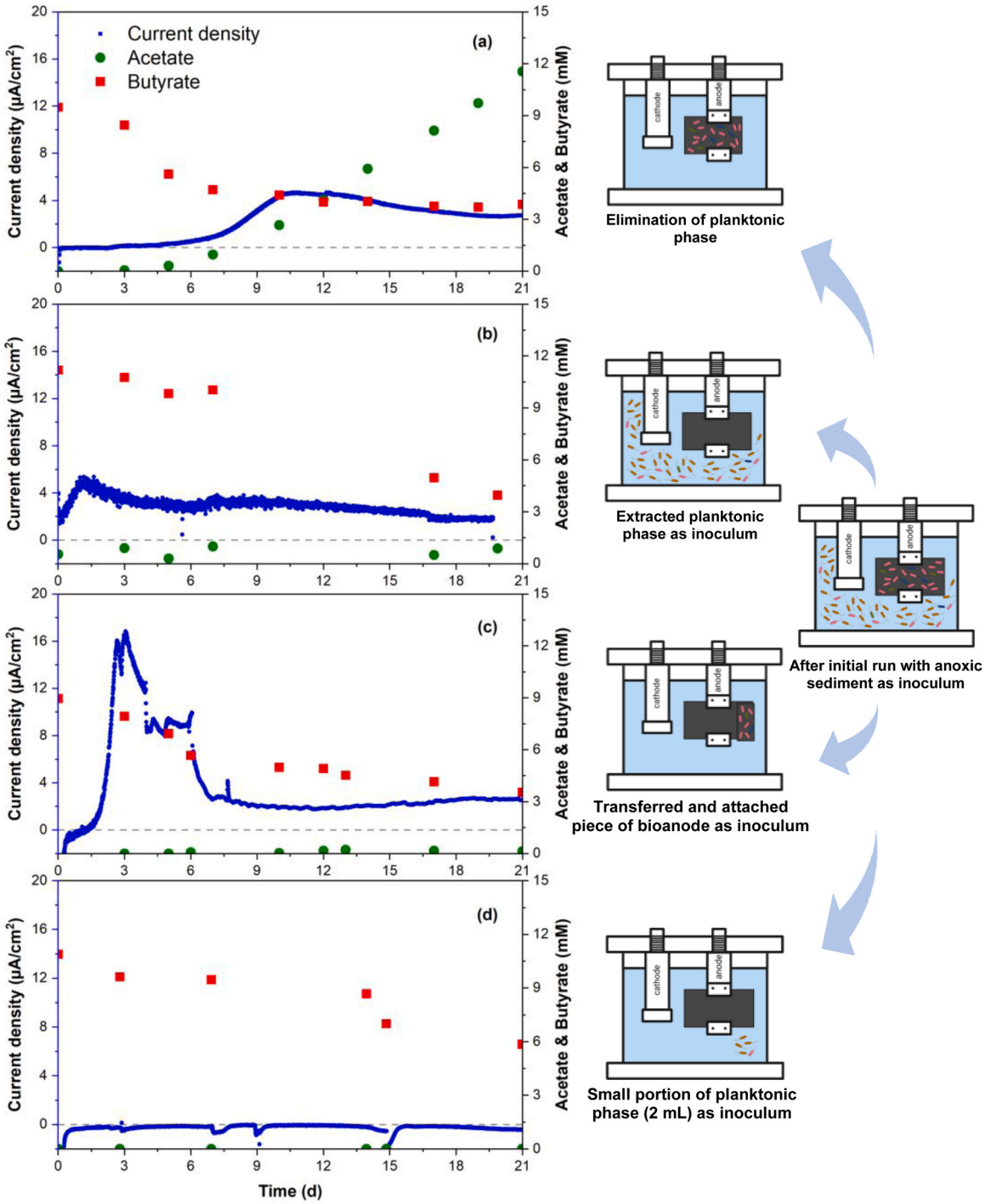

Fig. 2. The time course of current density, acetate, and butyrate in bioelectrochemical systems (BESs) inoculated with enriched bioanode (a), planktonic cells (b), small piece of bioanode (c), and only 2 mL of planktonic cell (d). The used bioanode and planktonic cells were harvested from a BES initially inoculated with sediment and run for ~50 days. All BESs were fed with sterile butyrate-based medium. (For interpretation of the references to color in this figure legend, the reader is referred to the web version of this article.).

3. Results and discussion

3.1. Response of inoculum from different origins

For the aim to seek butyrate-based exoelecrogenic microorganisms, inoculum form three different origins, i.e., cow manure, hydrolysis sludge, and anoxic sediment, were separately tested in identical BESs and compared according to the resulting profiles of current density, butyrate, and acetate (Fig. 1). The figure shows that significant butyrate degradation was visible in all BESs within the first 30 days. However, no significant current was generated in BESs inoculated with cow manure (Fig. 1a) or hydrolysis sludge (Fig. 1b). The re-addition of butyrate to such two BESs further resulted in the same observation, which could be attributed to non-exoelectrogenic side reactions, such as those towards methanogenesis. In contrast, in the BES inoculated with anoxic sediment

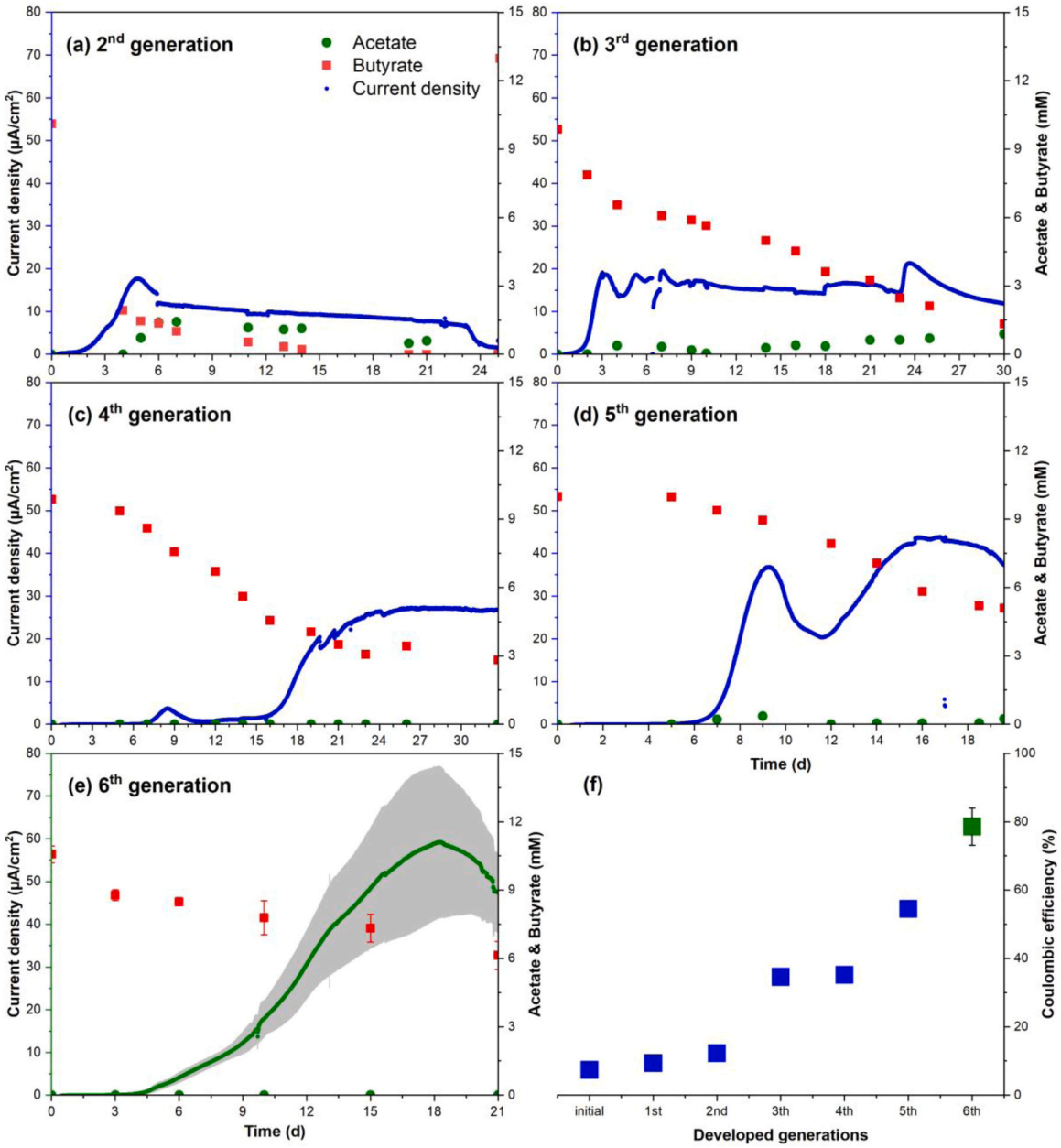

Fig. 3. The time course of current density, acetate, and butyrate in bioelectrochemical systems (BESs), where each one was inoculated with a piece of bioanode attached to its fresh anode generating five consecutive generations (a-e), and the relevant coulombic efficiency (CE) (f). The CE of BESs initially inoculated with sediment and 1st generation (used to examine the enrichment strategy) are also included. All BESs were fed with sterile butyrate-based medium. (For interpretation of the references to color in this figure legend, the reader is referred to the web version of this article.).

(Fig. 1c), the current density started to develop from day 16 and reached the peak of 23 μA/cm^2 at day 30. Such observed long lag-phase can be attributed to the initial establishment of biofilm along with the competing side reactions from the diverse planktonic cells existing in the system. The resulting CE of this initial run of BES inoculated with anoxic sediment was 7.42 %. This finding confirms the presence of exoelectroactive microorganisms, particularly on the anodic surface, which can be further enriched to improve the generated current and CE of the BES. Overall and given the results obtained from the three BESs, this experiment emphasizes the key role of inoculum origin in operating the bioprocess of interest, particularly during the startup period.

3.2. *Efficiency of proposed enrichment strategy*

Examination of the most electroactive portion of the microbial community initially enriched from the anoxic sediment (Fig. 1c) was performed by testing of four portions, i.e., initial bioanode (Fig. 2a), initial planktonic cells and fresh anode (Fig. 2b), a piece from initial bioanode attached to a fresh one (Fig. 2c), and 2 mL of initial planktonic cells and fresh anode (Fig. 2d). This was to identify which portion is more suitable for further enrichment to maximize the BES efficiency. The results obtained show clearly that inoculation with 2 mL of planktonic cells did not correlate with current generation; however, half of the butyrate content was consumed (Fig. 2d). This indicates the high potential of having side reactions in case improper enrichment was employed. In contrast, current generation was detected from the other three portions used for inoculation, where shorter lag-phases were determined in BESs started with fresh anodes (Figs. 2a, 2b, and 2c). This can be potentially attributed to the higher available surface area, and less competition with other physically attached microbes, for exoelectrogens to grow while performing EET. Although similar butyrate profiles were observed among these three inoculations, the one inoculated with a piece of bioanode had much higher maximum current density of 17.5 μA/cm^2 (Fig. 2c). Consistently, the corresponding CE slightly increased from 7.4 % to 9.4 % as compared with the initial inoculation with anoxic sediment. This can be explained by the selective enrichment of exoelectrogens existing on the anodic surface resulting in more active biofilm composition, which leads to a higher BES efficiency, particularly at the startup period.

Accordingly, consecutive transfers of a piece of bioanode were additionally employed for the aim of enriching exoelectrogens that particularly grow on the electrode surface. Maximizing the current density and CE was taken as an indicator, which resulted in six generations in total (Fig. 3). The BESs of the different generations were operated until reaching maximum current density. Although Figs. 3a and 3b show no increase in maximum current density of ~20 μA/cm^2 between the 2nd and 3rd generations, CE improved substantially from 12.3 % to 34.6 % indicating more efficient EET, however, with relatively slow kinetics. Afterwards, in the 4th to 6th generations, the observed longer lag-phases were a result of the bioanode piece being stored at −80°C before being transferred. However, the lag-phase, maximum current density, and CE substantially improved from the 4th to 6th generation (Figs. 3c and 3f). The 6th generation achieved maximum current density of 60 μA/cm^2 at a corresponding high CE of 78.6 %. Given the thermodynamics related to the potential anoxic butyrate oxidation pathway, it could be assumed that syntrophic interactions play a role in the process, as shown in Eqs. 2–3 (Müller et al., 2010).

$$\text{Butyrate} + 2H_2O \rightarrow 2\ \text{Acetate} + 2\ H_2 + H^+ \ (\Delta G^{0'} = +48.3\ \text{kJ/mol}) \quad (2)$$

$$H_2 + 2CO_2 \rightarrow \text{Acetate} + 2\ H_2O \ (\Delta G^{0'} = -101.4\ \text{kJ/mol}) \quad (3)$$

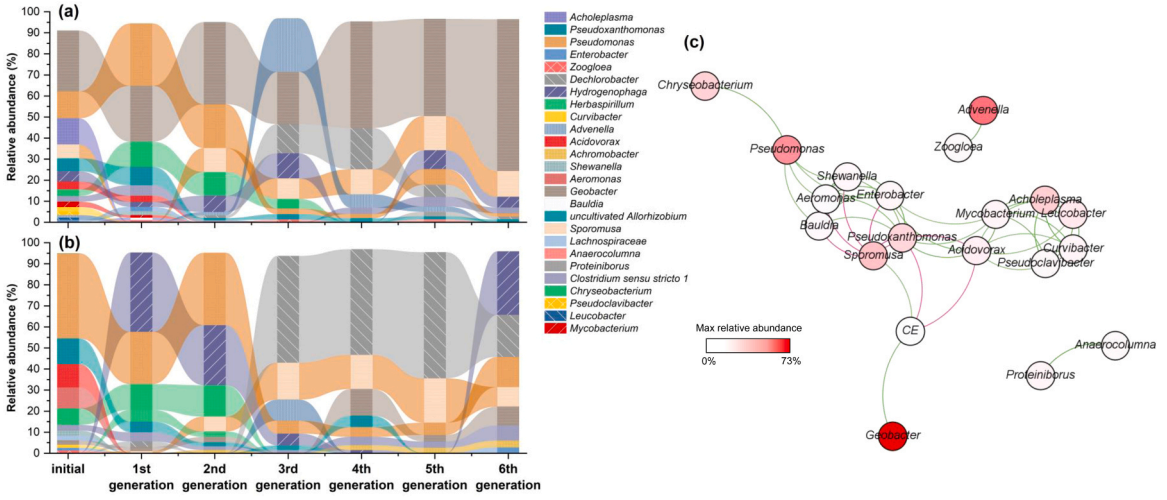

Fig. 4. Relative abundance of microorganisms, at genus level, for anodic (a) and planktonic samples (b), which were extracted from each generation in the enrichment procedure. The "initial" samples were collected at end of the initial run of bioelectrochemical system (BES) when inoculated with sediment. (c) Spearman-correlation network for the anodic microorganisms and associated coulombic efficiency (CE) at each generation; only significant correlations ($p<0.05$) are shown; green and red edges represent positive and negative correlations, respectively. (For interpretation of the references to color in this figure legend, the reader is referred to the web version of this article.).

Then, the question is how this relates to the observed anodic EET where two hypotheses can be considered, separately or in combination. First, a multistep reaction where acetate would be provided, by a syntrophic candidate, to serve as a substrate for exoelectrogens. Meanwhile, the acetate accumulation observed at 2nd and 3rd generations, along with similar butyrate profile, could be explained by less efficient exoelectrogens, which was not the case from the 4th generation onwards. Second, a one-step reaction where syntrophic and exoelectrogens would compete for the substrate (i.e., butyrate). For this, the microbial/molecular analyses below give more insights into the potential mechanisms. In summary, employing physiological selection could lead to the successful displacement of side reactions, thereby promoting the enrichment of exoelectrogens.

3.3. Microbial composition of the enriched cultures

Figs. 4a and 4b show the relative abundance of bacteria at genus level in samples collected from the planktonic phases and bio-anodes at each of the developed generations during the enrichment, starting from the BES inoculated with anoxic sediment (i.e., initial). The figures show that genus *Geobacter* gradually dominated the anodic samples with an increasing abundance from 29 % (initial) to 72 % (6th generation). *Geobacter* is the most characteristic genus among exoelectrogenic microorganisms and has been widely found to dominate anodic enrichments (Bond and Lovley, 2003). This finding emphasizes that *Geobacter* is the key player among the enriched microbes to perform EET. It is also interesting to note that abundance of genus *Sporomusa* was generally increasing through generations in both anodic (6.6–16 %) and planktonic samples (1.1–21 %). Genus *Sporomusa* has been described as chemo-lithotrophic microorganisms, with high capability of acetate assimilation via the reductive acetyl-CoA pathway (Wood-Ljundahl), which was a basis for several microbial electrosynthesis (MES) applications (Breznak, 2006; Nevin et al., 2010; Thatikayala and Min, 2021). With the potential availability of H_2 as by-product from the oxidation of butyrate to acetate (Eq. 2), presence of *Sporomusa* may indicate a synergistic role alongside *Geobacter*. Mixotrophic H_2 utilization with C1-compounds such as methanol and formate has also been described, suggesting membership in fermentative communities (Breznak, 2006). Further, a similar syntrophic consortium composed of *Sporomusa* and *Geobacter* was reported in methanol-fed single-chamber MFCs, where methanol was converted into acetate by *Sporomusa* (Kouzuma et al., 2018).

Concerning the planktonic community, dominant genera besides *Sporomusa*, particularly from the 3rd to 6th generations, were *Dechlorobacter* (20–60 %) and *Pseudomonas* (4.6–14.3 %). These genera have been widely found in BESs with potentials for mediated electron transfer (MET) as well as capabilities to deal with various organic compounds that might be existing, also in this experiment, due to cell-lysis (Khan et al., 2021; Song et al., 2020; Wu et al., 2019). In addition, genus *Hydrogenophaga* showed high abundance in the 6th generation (i.e., 30 %); given its function as H_2-oxidizing bacteria, this can also support the abovementioned H_2-availability for *Sporomusa*.

To understand and visualize the potential correlations among microorganisms in anodic/planktonic samples also with the corresponding CE, network analysis based on spearman-correlation ($p<0.05$) was conducted. Fig. 4c shows the network using only anodic samples and corresponding CE where significant positive correlations between CE and *Geobacter* as well as *Sporomusa* could be noticed. On the contrary, the network constructed using planktonic samples and CE did not result in any significant correlations between bacteria and CE, which emphasizes the minor role of planktonic community on the BES efficiency (Fig. S2). Further, the constructed network for microbes among anodic/planktonic samples did not show correlations with *Geobacter* (Fig. S3). These findings support the key role of *Geobacter* in the electrons-uptake efficiency from butyrate oxidation, along with the lower dependency on microorganisms existing in the planktonic phase. In addition, the indirect negative correlation found between Pseudomonas and CE (in anodic samples; Fig. 4c), the direct negative correlations with *Sporomusa*, and the positive correlations with several other genera highlight its irrelevant/competing role in the process. Various biodiversity indices were estimated to highlight the impact of employed transferring on both anodic and planktonic cultures, i.e., Shannon, Simpson, α-diversity, evenness, and Chao1 (Table 1). The results show that the observed OTUs behaved differently starting from the 3rd generation, which is consistent with the corresponding change in composition. Indices dynamics also show that the biodiversity of anodic communities was affected substantially due to the successive

Table 1
Major biodiversity indices of the identified microbial communities (at genus level) from samples collected from anode and planktonic phase during the enrichment process.

Indices	Sample	Enrichment generations						
		initial	1st	2nd	3rd	4th	5th	6th
Observed OTUs	anodic	31427	38498	37729	34730	33630	40498	60771
	planktonic	29396	32191	34571	22375	28194	29368	38055
Shannon	anodic	2.218	1.878	1.633	1.864	1.371	1.686	0.924
	planktonic	1.867	1.672	1.626	1.387	1.497	1.115	1.833
Simpson	anodic	0.843	0.792	0.748	0.816	0.655	0.721	0.421
	planktonic	0.768	0.750	0.747	0.652	0.679	0.551	0.810
α-diversity	anodic	1.524	1.159	0.844	0.850	0.648	0.940	0.610
	planktonic	1.193	0.858	0.852	0.677	0.763	0.554	0.740
evenness	anodic	0.819	0.756	0.743	0.848	0.705	0.732	0.475
	planktonic	0.751	0.761	0.740	0.713	0.720	0.622	0.881
Chao1	anodic	15	12	9	9	7	10	7
	planktonic	12	9	9	7	8	6	8

transfers compared to planktonic communities. This further confirms the minor role derived by the planktonic culture. The anodic samples were less diverse over the generations, supporting the intended functional selection.

3.4. Metagenomic/transcriptomic data and potential metabolic pathway

To elucidate the key organisms significantly involved in the process and to dissect the functional physiological interactions, metagenomic and transcriptomic analyses were performed only for the anodic biofilm of the 6th generation. Table S3 shows the main assembly statistics obtained while analyzing the raw data of Illumina sequencing. Meanwhile, 94.8 % of the processed reads could be assigned to the domains of bacteria, archaea, and eukaryota where bacteria were nearly the sole existing organisms (Table S4). Then, with respect to the aimed metatranscriptomic analysis, the assembly of individual genomic bins was performed to be used as a reference for mapping the RNA-sequencing reads. Processed by the Metabat and CheckM algorithms embedded in SqueezeMeta pipeline, five genome bins were assembled covering 72.8 % of the metagenome reads (Table 2). The table also shows that the identified genera are comparable with the dominant ones obtained from the 16S rDNA amplicon sequencing shown earlier in Fig. 4. To obtain further information at the species level for *Geobacter*, the most abundant genus, the identified 16S rDNA segments were subjected to an external search using the Nucleotide Basic Local Alignment Search Tool (BLAST) available at NCBI. This resulted in the identification of the strains *Geobacter bemidjiensis* Bem (99.7 % identity) and *Geobacter bremensis* Dfr1 (98.2 % identity) (Table S5 and Fig. S4). As reported earlier, these two species are capable of coupling the reduction of Fe^{3+} or Mn^{4+} with the oxidation of butyrate and a variety of other carbon compounds (Nevin et al., 2005). However, to date, evidence of electrode reduction for *Geobacter bremensis* Dfr1 (and not for *Geobacter bemidjiensis* Bem) have been reported (Aklujkar et al., 2010; Nevin et al., 2005). In addition, the previous exclusion of *Geobacter bemidjiensis* Bem in relation to the electrode was not fully justified, as it lacked supporting data at the gene level. Therefore, further isolation studies are needed to confirm the responsible strain(s).

To use the transcriptions data to study the potential pathways involved in the bioanodic oxidation of butyrate, functional biomarkers of butyrate oxidation, acetate metabolism, C1-metabolism and key anabolic enzymes were targeted (Figs. 5a and 5b). The potential *c*-type cytochromes involved in EET were identified bioinformatically, using heme recognition sequences (CXXCH) of the translated genes as markers. The genes expressions of the respective genomic bins, as TPM, are heat-mapped as shown in Fig. 5a (using logarithmic color scale). First, when concerning the central butyrate oxidation route, high expression levels of 335, 154, and 385 TPM were determined for the *buk*, *ptb*, and *cs* genes, respectively. As most of these expressions were assigned to *Geobacter*, this emphasizes its functional role in the oxidative process. Further, with inclusion of the highly expressed multi-heme *c*-type cytochromes (>5550 TPM), as key proteins for EET, the anodic reduction can most likely be solely assigned to *Geobacter*. This could also be supported by the lack of expressions found for common mediated electron transfer (MET) pathways, such as flavin or phenazine synthesis (Fig. 5a).

Second, for the claimed involvement of acetate assimilation from H_2 and CO_2 by *Sporomusa*, followed by anodic oxidation of acetate via other organisms, expressions of relevant genes were checked (Figs. 5a and 5b). Concerning the assimilation of acetate, the hydrogenotrophic CO_2 fixation is limited by the oxidation-sensitive carbon monoxide-dehydrogenase/acetyl-CoA synthase complex (*acsA/B*), which condenses the formed methyl and carbonyl groups to acetyl-CoA (Breznak, 2006). Subsequent cleavage of high-energy thioester binding and substrate chain phosphorylation is then catalyzed by phosphate acetyltransferase (*pta*) and acetate kinase (*ack*). High expression levels for the complex *acsA/B* (16.5 TPM), *pta* (7.81 TPM), and *ack* (7.78 TPM) were associated with *Sporomusa* (Fig. 5a). Moreover, the complex of heterodisulfide reductase (*hdrA/B/C*) was highly expressed by *Sporomusa* (46.4 TPM); such complex is significantly involved in the reduction of CO_2 by methanogens and acetogens (Mock et al., 2014). Further, for the carbonyl branch of the Wood-Ljundahl (WL) pathway, the NADP-reducing hydrogenase complex (*hndBCD*) was expressed mainly by *Sporomusa* (15.1 TPM), providing NADP for the reduction of CO_2 (Figs. 5a and 5b) (Poehlein et al., 2012; Wong et al., 2018). Afterwards, concerning the biomarkers of following acetate uptake, *Geobacter* unsurprisingly showed high expression levels for *ack* (1266 TPM), *pta* (502 TPM), succinyl:acetate CoA transferase (*ato-1*; 311 TPM), and acetyl-CoA synthetase (*acs*; 1115 TPM). Moreover, high expression of the two hydrogenases *hyaA* (49 TPM) and *mvhD* (6.4 TPM) were exclusively associated with *Geobacter*. The high expression of *hya* was reported earlier to be attributed to excess metabolism in *G. sulfurreducens* (Coppi, 2005). In the meantime, the role of the other organisms (i.e., *Clostridium*, *Pseudomonas*, and family Comamonadaceae) seems minor based on the selected biomarkers.

Overall, these findings provide a mechanistic insight into the physiological relationships within the obtained anodic butyrate oxidation. In combination with the 16S rDNA results, *Geobacter* genus can be considered as the key player of the anodic butyrate oxidation. Moreover, a beneficial syntrophic interaction between *Geobacter* and *Sporomusa* is suggested, where a postulated excess metabolism by *Geobacter* could allow *Sporomusa* to coexist (Fig. 5c). Excess metabolism represents a physiological event in Eukaryotes/prokaryotes, where incomplete substrate oxidation occurs despite the sufficient electron accepting capacity with acetyl-CoA catalyzed

Table 2
Classification and statistics of the taxonomic bins obtained from the metagenomic data analysis of the enriched anodic microbial community.

Bins	Length (bp)	Contigs contamination (%)	Completeness (%)	Binscontamination (%)	Reads	
					number	%
Family Comamonadaceae	3546,209	0.08	91.6	3.58	1730,018	5,17
Genus *Sporomusa*	4179,737	0.344	89.2	1.70	876,180	2,62
Genus *Pseudomonas*	7453,089	0.657	84.4	39.7	339,726	1,01
Genus *Clostridium*	1264,037	0	69.5	0.83	668,807	2,00
Genus *Geobacter*	2171,900	0	52.3	8.32	20,738,639	62,02

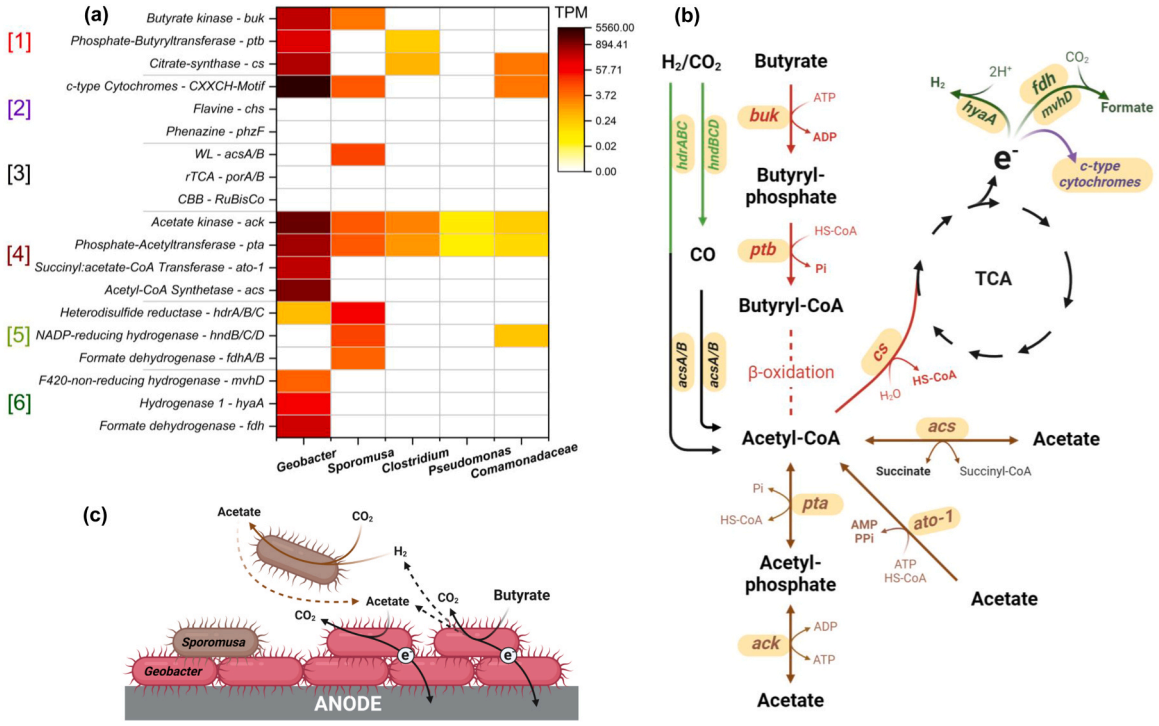

Fig. 5. (a) A TPM-based heatmap for the potential key biomarkers involved in anodic butyrate oxidation; only results for the abundant organisms obtained by metagenomic analysis are included; logarithmic color scale is used. The six functional pathways of interest (i.e., 1–6) were butyrate oxidation, extracellular electron transfer, C1-metabolism, acetate oxidation, hydrogen/formate consumption, and hydrogen/formate production, respectively. (b) Schematic diagram showing the representative genes and associated potential pathways. (c) Schematic diagram presenting the proposed bioanodic reactions via *Geobacter* and *Sporomusa*. TPM, Transcripts per million kilobase; WL, "Wood-Ljungdahl" pathway; rTCA, reductive tricarboxylic acid cycle; CBB, Calvin–Benson–Bassham cycle. (For interpretation of the references to color in this figure legend, the reader is referred to the web version of this article.).

to acetate and ATP molecule (Szenk et al., 2017); meanwhile, the intracellular acetyl-CoA accumulation, associated with repression of the TCA cycle or limitations in electron transfer, could lead to such event (Majewski and Domach, 1990; Zhuang et al., 2011). Accordingly, in this study, such intracellular imbalance could result in the formation of acetate and hydrogen, corresponding with a CE decline (electrons loss due to H_2 outgassing) only in case no efficient H_2-recycling means exist, e.g., *Sporomusa*. Still, it cannot be conclusively determined which type of interaction is involved, where IET based on H_2, formate, and/or direct interspecies electron transfer (DIET) can be established between the two genera.

3.5. *Boosting efficiency via bio-augmentation using G. sulfurreducens*

Given the above-mentioned hypothesis to have acetate and H_2 as major intermediates during the anodic oxidation of butyrate, the inclusion of *G. sulfurreducens*, which in addition to acetate also uses hydrogen to gain electrons, was examined. In addition, the bioaugmentation using *G. sulfurreducens* proved earlier to also improve the respiratory capacity between microorganisms and electrode (Schmidt et al., 2018). Therefore, two separate triplicates using the last generation of enrichment were run for a month, where *G. sulfurreducens* was introduced (OD_{600} of 0.1) into the bulk liquid phase of one of them for comparison. As shown in Figs. 6a–6b, no significant changes were found between both butyrate oxidation and acetate production/consumption kinetics in both cases. However, 31–41 % improvements in current density (maximum and mean) as well as CE were obtained due to adding *G. sulfurreducens* (Figs. 6d–6e). Altogether, these findings indicate more efficient use of the intermediates of butyrate oxidation rather than improving the butyrate elimination rate. Theoretically, the complete anodic oxidation of butyrate to CO_2 (with 2 moles of acetate and 2 moles of H_2, as intermediates) yields 20 electrons of which 16 electrons (80 %) can be gained from acetate and 4 electrons (20 %) from H_2. Accordingly, and given the obtained CE values of ~80 % and ~100 % for the enriched culture without and with *G. sulfurreducens*, respectively, it can be speculated that such improvement was due to a more efficient H_2-recycling as an additional electron donor. This may also indicate a higher affinity for H_2 by *G. sulfurreducens*, in case acetate is also available, as compared to *Sporomusa*. Likewise, the syntrophic interaction between *G. sulfurreducens* and the butyrate oxidizer *Syntrophomonas wolfei* in a BES was found to be more efficient than that between *S. wolfei* and methanogens (Wang et al., 2023). Eventually, this experiment provides further evidence for the hypothesized interaction between *Geobacter* and *Sporomusa* in the enriched butyrate-oxidizing culture; moreover, it emphasizes that enhanced metabolic cooperation and overall physiological suitability for targeted BESs, can be obtained via including

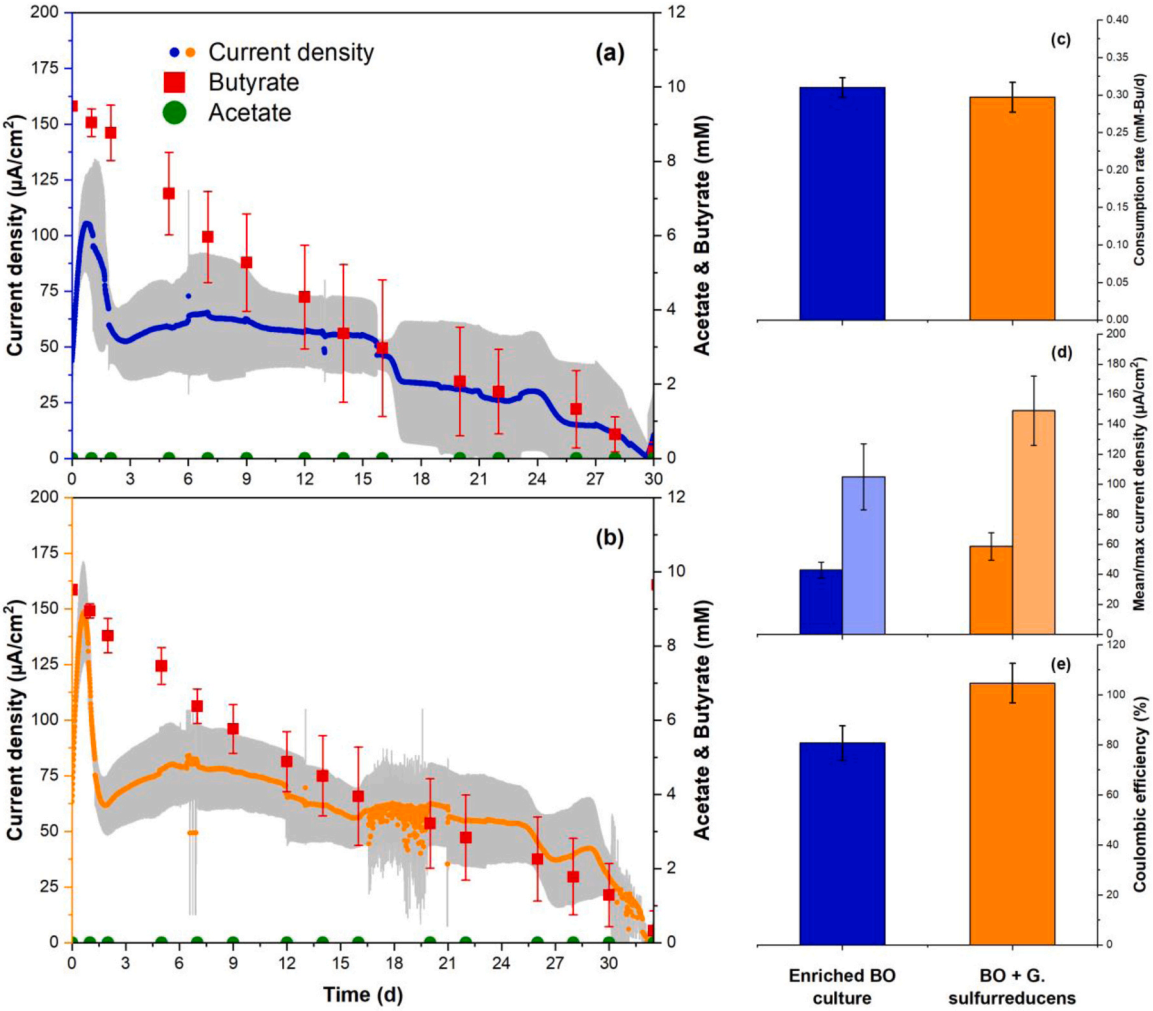

Fig. 6. The time course of current density, butyrate, and acetate in bioelectrochemical systems (BESs) fed with butyrate, as sole electron donor, and inoculated with the enriched butyrate-oxidizing culture (BO) solely (a), and bioaugmented with *G. sulfurreducens* at OD_{600} of 0.1 (b); the associated butyrate consumption rate (c), mean and maximum (faded) current density (d), and coulombic efficiency (CE) (e). (For interpretation of the references to color in this figure legend, the reader is referred to the web version of this article.).

G. sulfurreducens.

3.6. BES efficiency when using butyrate-rich hydrolysate

Herein, the enriched butyrate-oxidizing community bioaugmented with *G. sulfurreducens* was examined, in a FP-BES, with real fermentation hydrolysate to validate its efficiency for industrial applications. As shown in Fig. 7, first, a startup period of 14 days was employed using the usual growth medium spiked with a mixture of butyrate, acetate, and propionate at a concentration of 10 mM each. As expected, when *G. sulfurreducens* is a biocatalyst in BESs, rapid consumption of acetate was observed. Butyrate and propionate were further consumed at a lower rate and the maximum obtained current density was ~130 μA/cm^2, which was comparable with values recorded for only butyrate as sole substrate. These findings highlight that (1) the enriched culture is able to oxidize propionate in addition to butyrate and acetate, and (2) *G. sulfurreducens* showed robustness against initial load of propionate and butyrate (10 mM), which is in agreement with our earlier study (Härrer et al., 2022). Second, the hydrolysate was gradually pumped into the 200 mL-reservoir attached to the FP-BES, until full replacement. The related results in Fig. 7 show that the culture rapidly reacted to the hydrolysate with maximum current density of ~350 μA/cm^2 indicating a significant robustness of the anodic culture. However, the accumulation of organic acids (>15 mM) caused a gradual deterioration in current density until reaching 160 μA/cm^2 where acetate, butyrate, and propionate concentrations reached ~30 mM. At this point, the observed organic acids comprised ~50 % of the DOC content; moreover, the DOC profile during the whole experiment indicates that organics other than acetate, butyrate, and propionate are consumed (Fig. 7). This could be attributed to the still existence of various fermentative bacteria within the enriched culture that can interact with the real hydrolysate matrix.

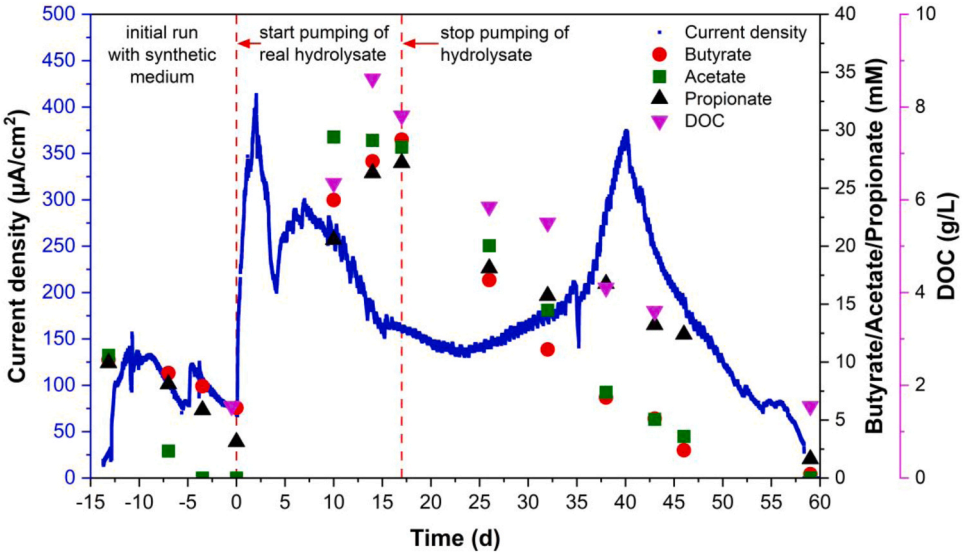

Fig. 7. The time course of current density, butyrate, acetate, propionate, and dissolved organic-carbon (DOC) in a bioelectrochemical system (BES) inoculated with the enriched butyrate-oxidizing culture and fed with real fermentation hydrolysate. Negative X-axe values represent a startup period when the BES was fed with synthetic medium composed of acetate, propionate, and butyrate. (For interpretation of the references to color in this figure legend, the reader is referred to the web version of this article.

Afterwards, pumping the hydrolysate was stopped, and the FP-BES was switched into batch-mode operation. The development in current generation (started at day 33), particularly when the organic acids concentrations went below 15 mM, further emphasizes the stress conditions induced by the high and complex organic load. The maximum obtained current density was nearly the same as observed during the hydrolysate pumping-phase. It can also be noticed that the increase in current density corresponded with lower propionate kinetics compared to acetate and butyrate, which emphasizes the more efficient anodic electron uptake from butyrate and acetate. Meanwhile, a high overall CE of 86.9 % (based on DOC) was obtained for the process during this experimental phase (day 17 to day 59; Fig. 7). By looking at previous studies on the bioelectrochemical oxidation of butyrate, it was found that most of them were under the configuration of MFC (Table 3). It can be noticed that mainly mixed cultures, especially from WWTPs were used, which

Table 3
Previous results of bioelectrochemical systems (BESs) dealing with butyrate as sole electron donor.

Butyrate concentration	Reactor / operational conditions	Current density / productivity	Coulombic efficiency (%)	Inoculum	Ref.
0.9 g/L(1 g-COD/L)	Flat-plate MFC	270 mW/m^2	50	Mixed culture	(Min and Logan, 2004)
1 g/L	Single chamber membraneless MFC1000 Ω	0.77 A/m^{2}305 mW/m^2	5	Mixed culture	(Liu et al., 2005)
0.4 g/L	FP-like MFC20–100 Ω	0.95 A/m^2-membrane	46–67 (COD)[a]	Mixture from different sources	(Freguia et al., 2010)
0.6 g/L(7 mM)	H-type MFC500 mV/1000 Ω	-	19	Mixed culture (anaerobic; WWTP)	(Zhang et al., 2011)
0.45 g/L(0.5 g-COD/L)	Air-cathode MFC80–100 Ω	836 mW/m^2	56	Mixed culture(WWTP)	(Yu et al., 2015)
1.5–3.5 g/L	H-type MFC350 mV/1000 Ω	450 mV(output voltage)	-	*S. wolfei* with *G. sulfurreducens*	(Wang et al., 2023)
0.4 g/L(5 mM)	H-type MEC100 mV (vs SHE)	0.16 A/m^2	-	Mixed culture (WWTP)	(Torres et al., 2007)
0.7 g/L(0.8 g-COD/L)	FP-like MEC1000 mV/10 Ω (initial acetate-feed)	1.25 A/m^2	72 (COD)[a]	Mixed culture froma running MEC	(Yang et al., 2015)
1 g/L	Single chambermembraneless MEC800 mV	0.27 A/m^2	50	Mixed culture(acetate-fed MEC)	(Varanasi and Das, 2020)
2.3 g/L	Single chambermembraneless MEC500 mV	0.2 A/m^2	-	Mixed culture (Anaerobic fermenter)	(Zhang et al., 2022)
0.9 g/L(10 mM)	C-BES (MEC)AP of 0 mV (vs SHE)	1.1–1.5 A/m^2	>80	enriched BO w/o *G. sulfurreducens*	This study
30+30+25 mM Bu/Pr/Ac (real hydrolysate)	FP-BES (MEC)AP of 0 mV (vs SHE)	3.5 A/m^2	87 (DOC)[a]	enriched BO with *G. sulfurreducens*	This study

[a] Coulombic efficiency was calculated based on COD or DOC variations; C-BES, cylindrical bioelectrochemical system; Bu, butyrate; Pr, propionate; Ac, acetate; MFC, microbial fuel cell, MEC, microbial electrolysis cell; BO, butyrate-oxidizers; AP, anode potential.

stresses the potential role of other inoculum sources according to the targeted process. In addition, studies using the flat-plate configuration showed high CEs, emphasizing the flow pattern impact on BESs. As compared to the present study, lower CEs of 5–72 % were previously reported, in which the maximum CE of 72 % (and corresponding current of 1.25 A/m^2) was achieved at a higher cell-voltage of 1 V (Yang et al., 2015).

Eventually, achieving such high CEs when using butyrate (as the sole electron donor) and then butyrate-rich hydrolysate highlights the significance of the proposed approach, where efficient enrichment of exoelectrogens was a game changer. This approach, meanwhile, opens up opportunities to advance the applicability of BESs as a means of energy recovery from waste. However, certain limitations still require future investigation, such as testing the approach with other longer-chain fatty acids abundant in some hydrolysates (e.g., valerate and oleate), assessing the long-term stability of performance under continuous-mode operations using hydrolysates, and developing strategies for the periodic reactivation of the anodic biofilm while eliminating planktonic cells in operating BESs.

4. Conclusions

Prior enrichment of exoelectrogens solely on butyrate proved to be a successful strategy to upgrade the performance of BESs dealing with butyrate-rich effluents. Elimination of potential anode-competing reactions was achieved via consecutively transferring a piece from the enriched bioanode to be attached to fresh electrodes, as active inoculum, until reaching maximum CE. Gene expression analysis showed that EET from butyrate to the anode likely goes through acetate and H_2, with *Geobacter* (most likely *G. bemidjiensis* Bem and/or *G. bremensis* Dfr1) being responsible, in cooperation with *Sporomusa* consuming excess H_2. Additionally introducing *G. sulfurreducens* to the enriched culture further accelerated acetate oxidation, resulting in improved CE also when tested with real hydrolysate as substrate. Overall, this approach provides guidance to address the applicability limitations that are to-date associated with BESs.

CRediT authorship contribution statement

Ahmed Elreedy: Writing – original draft, Visualization, Validation, Methodology, Investigation, Formal analysis, Data curation. **Daniel Härrer:** Visualization, Validation, Methodology, Investigation, Formal analysis, Data curation, Conceptualization. **Johannes Gescher:** Writing – review & editing, Supervision, Resources, Project administration, Methodology, Funding acquisition, Formal analysis, Conceptualization. **Rowayda Ali:** Writing – review & editing, Validation, Methodology, Investigation, Formal analysis, Data curation. **Andrea Hille-Reichel:** Writing – review & editing, Validation, Methodology, Investigation, Formal analysis, Data curation.

Declaration of Competing Interest

The authors declare that they have no known competing financial interests or personal relationships that could have appeared to influence the work reported in this paper.

Acknowledgements

This work was financially supported by the German Federal Ministry of Education and Research (BMBF) (grant number: 031B0365A [RECICL project] and 031B1053D [BROWSE project]). The authors gratefully thank Kerzenmacher's research group (University of Bremen, Germany) for providing the flat-plate bioelectrochemical system (FP-BES) used in this study.

Appendix A. Supporting information

Supplementary data associated with this article can be found in the online version at doi:10.1016/j.eti.2024.103871.

Data Availability

The data that has been used is confidential.

References

Aklujkar, M., Young, N.D., Holmes, D., Chavan, M., Risso, C., Kiss, H.E., Han, C.S., Land, M.L., Lovley, D.R., 2010. The genome of geobacter bemidjiensis, exemplar for the subsurface clade of geobacter species that predominate in Fe(III)-reducing subsurface environments. BMC Genom. 2010 111 11, 1–18. https://doi.org/10.1186/1471-2164-11-490.

Ali, R., Saravia, F., Hille-Reichel, A., Härrer, D., Gescher, J., Horn, H., 2021. Enhanced production of propionic acid through acidic hydrolysis by choice of inoculum. J. Chem. Technol. Biotechnol. 96, 207–216. https://doi.org/10.1002/jctb.6529.

Baudler, A., Riedl, S., Schröder, U., 2014. Long-term performance of primary and secondary electroactive biofilms using layered corrugated carbon electrodes. Front. Energy Res. 2, 85812. https://doi.org/10.3389/fenrg.2014.00030.

Blanchet, E., Desmond, E., Erable, B., Bridier, A., Bouchez, T., Bergel, A., 2015. Comparison of synthetic medium and wastewater used as dilution medium to design scalable microbial anodes: application to food waste treatment. Bioresour. Technol. 185, 106–115. https://doi.org/10.1016/j.biortech.2015.02.097.
Bond, D.R., Lovley, D.R., 2003. Electricity production by geobacter sulfurreducens attached to electrodes. Appl. Environ. Microbiol. 69, 1548–1555. https://doi.org/10.1128/AEM.69.3.1548-1555.2003.
Breznak, J.A., 2006. The Genus Sporomusa. Prokaryotes 991–1001. https://doi.org/10.1007/0-387-30744-3_34.
Brunner, S., Klessing, T., Dötsch, A., Sturm-Richter, K., Gescher, J., 2019. Efficient bioelectrochemical conversion of industrial wastewater by specific strain isolation and community adaptation. Front. Bioeng. Biotechnol. 7. https://doi.org/10.3389/fbioe.2019.00023.
Choi, Y., Kim, D., Choi, H., Cha, J., Baek, G., Lee, C., 2023. A study of electron source preference and its impact on hydrogen production in microbial electrolysis cells fed with synthetic fermentation effluent. Bioengineered 14, 2244759. https://doi.org/10.1080/21655979.2023.2244759.
Coppi, M.V., 2005. The hydrogenases of Geobacter sulfurreducens: a comparative genomic perspective. Microbiology. https://doi.org/10.1099/mic.0.27535-0.
Freguia, S., Teh, E.H., Boon, N., Leung, K.M., Keller, J., Rabaey, K., 2010. Microbial fuel cells operating on mixed fatty acids. Bioresour. Technol. 101, 1233–1238. https://doi.org/10.1016/j.biortech.2009.09.054.
Guang, L., Koomson, D.A., Jingyu, H., Ewusi-Mensah, D., Miwornunyuie, N., 2020. Performance of exoelectrogenic bacteria used in microbial desalination cell technology. Int. J. Environ. Res. Public Health. https://doi.org/10.3390/ijerph17031121.
Härrer, D., Elreedy, A., Ali, R., Hille-Reichel, A., Gescher, J., 2022. Probing the robustness of geobacter sulfurreducens against fermentation hydrolysate for uses in bioelectrochemical systems. SSRN Electron. J. 369, 128363. https://doi.org/10.2139/ssrn.4239421.
He, W., Wallack, M.J., Kim, K.Y., Zhang, X., Yang, W., Zhu, X., Feng, Y., Logan, B.E., 2016. The effect of flow modes and electrode combinations on the performance of a multiple module microbial fuel cell installed at wastewater treatment plant. Water Res. 105, 351–360. https://doi.org/10.1016/j.watres.2016.09.008.
Jing, X., Liu, X., Zhang, Z., Wang, X., Rensing, C., Zhou, S., 2022. Anode respiration-dependent biological nitrogen fixation by geobacter sulfurreducens. Water Res. 208, 117860. https://doi.org/10.1016/j.watres.2021.117860.
Khan, M.D., Li, D., Tabraiz, S., Shamurad, B., Scott, K., Khan, M.Z., Yu, E.H., 2021. Integrated air cathode microbial fuel cell-aerobic bioreactor set-up for enhanced bioelectrodegradation of azo dye Acid Blue 29. Sci. Total Environ. 756, 143752. https://doi.org/10.1016/j.scitotenv.2020.143752.
Klein, E.M., Knoll, M.T., Gescher, J., 2023. Microbe–anode interactions: comparing the impact of genetic and material engineering approaches to improve the performance of microbial electrochemical systems (MES). Microb. Biotechnol. 1–24. https://doi.org/10.1111/1751-7915.14236.
Kokko, M., Epple, S., Gescher, J., Kerzenmacher, S., 2018. Effects of wastewater constituents and operational conditions on the composition and dynamics of anodic microbial communities in bioelectrochemical systems. Bioresour. Technol. 258, 376–389. https://doi.org/10.1016/j.biortech.2018.01.090.
Kouzuma, A., Ishii, S., Watanabe, K., 2018. Metagenomic insights into the ecology and physiology of microbes in bioelectrochemical systems. Bioresour. Technol. 255, 302–307. https://doi.org/10.1016/j.biortech.2018.01.125.
Lin, L., Zakaria, B.S., Hosseini Koupaie, E., Bazyar Lakeh, A.A., Hafez, H., Elbeshbishy, E., Dhar, B.R., 2019. Evaluation of sludge liquors from acidogenic fermentation and thermal hydrolysis process as feedstock for microbial electrolysis cells. Int. J. Hydrog. Energy 44, 30031–30038. https://doi.org/10.1016/j.ijhydene.2019.09.162.
Liu, H., Cheng, S., Logan, B.E., 2005. Production of electricity from acetate or butyrate using a single-chamber microbial fuel cell. Environ. Sci. Technol. 39, 658–662. https://doi.org/10.1021/es048927c.
Logan, B.E., Regan, J.M., 2006. Microbial fuel cells—challenges and applications. Environ. Sci. Technol. 40, 5172–5180.
Logan, B.E., Wallack, M.J., Kim, K.Y., He, W., Feng, Y., Saikaly, P.E., 2015. Assessment of microbial fuel cell configurations and power densities. Environ. Sci. Technol. Lett. 2, 206–214. https://doi.org/10.1021/acs.estlett.5b00180.
Lovley, D.R., 2006. Bug juice: Harvesting electricity with microorganisms. Nat. Rev. Microbiol. https://doi.org/10.1038/nrmicro1442.
Madjarov, J., Prokhorova, A., Messinger, T., Gescher, J., Kerzenmacher, S., 2016. The performance of microbial anodes in municipal wastewater: pre-grown multispecies biofilm vs. natural inocula. Bioresour. Technol. 221, 165–171. https://doi.org/10.1016/j.biortech.2016.09.004.
Majewski, R.A., Domach, M.M., 1990. Simple constrained-optimization view of acetate overflow in E. coli. Biotechnol. Bioeng. 35, 732–738. https://doi.org/10.1002/bit.260350711.
Miceli, J.F., Garcia-Peña, I., Parameswaran, P., Torres, C.I., Krajmalnik-Brown, R., 2014. Combining microbial cultures for efficient production of electricity from butyrate in a microbial electrochemical cell. Bioresour. Technol. 169, 169–174. https://doi.org/10.1016/j.biortech.2014.06.090.
Min, B., Logan, B.E., 2004. Continuous electricity generation from domestic wastewater and organic substrates in a flat plate microbial fuel cell. Environ. Sci. Technol. 38, 5809–5814. https://doi.org/10.1021/es0491026.
Mock, J., Wang, S., Huang, H., Kahnt, J., Thauer, R.K., 2014. Evidence for a hexaheteromeric methylenetetrahydrofolate reductase in Moorella thermoacetica. J. Bacteriol. 196, 3303–3314. https://doi.org/10.1128/JB.01839-14.
Müller, N., Worm, P., Schink, B., Stams, A.J.M., Plugge, C.M., 2010. Syntrophic butyrate and propionate oxidation processes: from genomes to reaction mechanisms. Environ. Microbiol. Rep. https://doi.org/10.1111/j.1758-2229.2010.00147.x.
Nevin, K.P., Holmes, D.E., Woodard, T.L., Hinlein, E.S., Ostendorf, D.W., Lovley, D.R., 2005. Geobacter bemidjiensis sp. nov. and Geobacter psychrophilus sp. nov., two novel Fe(III)-reducing subsurface isolates. Int. J. Syst. Evol. Microbiol. 55, 1667–1674. https://doi.org/10.1099/ijs.0.63417-0.
Nevin, K.P., Woodard, T.L., Franks, A.E., Summers, Z.M., Lovley, D.R., 2010. Microbial electrosynthesis: feeding microbes electricity to convert carbon dioxide and water to multicarbon extracellular organic compounds. MBio 1 (4), 1. https://doi.org/10.1128/mBio.00103-10.Editor.
Pandey, P., Shinde, V.N., Deopurkar, R.L., Kale, S.P., Patil, S.A., Pant, D., 2016. Recent advances in the use of different substrates in microbial fuel cells toward wastewater treatment and simultaneous energy recovery. Appl. Energy. https://doi.org/10.1016/j.apenergy.2016.01.056.
Poehlein, A., Schmidt, S., Kaster, A.K., Goenrich, M., Vollmers, J., Thürmer, A., Bertsch, J., Schuchmann, K., Voigt, B., Hecker, M., Daniel, R., Thauer, R.K., Gottschalk, G., Müller, V., 2012. An ancient pathway combining carbon dioxide fixation with the generation and utilization of a sodium ion gradient for ATP synthesis. PLoS One 7, 33439. https://doi.org/10.1371/journal.pone.0033439.
Rainey, F.A., Fritze, D., Stackebrandt, E., 1994. The phylogenetic diversity of thermophilic members of the genus Bacillus as revealed by 16S rDNA analysis. FEMS Microbiol. Lett. 115, 205–212. https://doi.org/10.1111/j.1574-6968.1994.tb06639.x.
Riedl, S., Brown, R.K., Klöckner, S., Huber, K.J., Bunk, B., Overmann, J., Schröder, U., 2017. Successive conditioning in complex artificial wastewater increases the performance of electrochemically active biofilms treating real wastewater. ChemElectroChem 4, 3081–3090. https://doi.org/10.1002/celc.201700929.
Rossi, R., Hur, A.Y., Page, M.A., Thomas, A.O., Butkiewicz, J.J., Jones, D.W., Baek, G., Saikaly, P.E., Cropek, D.M., Logan, B.E., 2022. Pilot scale microbial fuel cells using air cathodes for producing electricity while treating wastewater. Water Res. 215, 118208. https://doi.org/10.1016/j.watres.2022.118208.
Schmidt, A., Sturm, G., Lapp, C.J., Siebert, D., Saravia, F., Horn, H., Ravi, P.P., Lemmer, A., Gescher, J., 2018. Development of a production chain from vegetable biowaste to platform chemicals. Microb. Cell Fact. 17, 90. https://doi.org/10.1186/s12934-018-0937-4.
Song, H.L., Lu, Y.X., Yang, X.L., Xu, H., Singh, R.P., Du, K.X., Yang, Y.L., 2020. Degradation of sulfamethoxazole in low-C/N ratio wastewater by a novel membrane bioelectrochemical reactor. Bioresour. Technol. 305, 123029. https://doi.org/10.1016/j.biortech.2020.123029.
Tamames, J., Puente-Sánchez, F., 2019. SqueezeMeta, a highly portable, fully automatic metagenomic analysis pipeline. Front. Microbiol. 10, 3349. https://doi.org/10.3389/fmicb.2018.03349.
Thatikayala, D., Min, B., 2021. Copper ferrite supported reduced graphene oxide as cathode materials to enhance microbial electrosynthesis of volatile fatty acids from CO2. Sci. Total Environ. 768, 144477. https://doi.org/10.1016/j.scitotenv.2020.144477.
Torres, C.I., Kato Marcus, A., Rittmann, B.E., 2007. Kinetics of consumption of fermentation products by anode-respiring bacteria. Appl. Microbiol. Biotechnol. 77, 689–697. https://doi.org/10.1007/s00253-007-1198-z.
Varanasi, J.L., Das, D., 2020. Maximizing biohydrogen production from water hyacinth by coupling dark fermentation and electrohydrogenesis. Int. J. Hydrogen Energy 45, 5227–5238. https://doi.org/10.1016/j.ijhydene.2019.06.030.
Wang, T., Kuang, B., Ni, Z., Guo, B., Li, Y., Zhu, G., 2023. Stimulating Anaerobic degradation of butyrate via syntrophomonas wolfei and geobacter sulfurreducens: characteristics and mechanism. Microb. Ecol. 85, 535–543. https://doi.org/10.1007/s00248-022-01981-2.

Wong, H.L., White, R.A., Visscher, P.T., Charlesworth, J.C., Vázquez-Campos, X., Burns, B.P., 2018. Disentangling the drivers of functional complexity at the metagenomic level in Shark Bay microbial mat microbiomes. ISME J. 12, 2619–2639. https://doi.org/10.1038/s41396-018-0208-8.

Wu, M., Xu, X., Lu, K., Li, X., 2019. Effects of the presence of nanoscale zero-valent iron on the degradation of polychlorinated biphenyls and total organic carbon by sediment microbial fuel cell. Sci. Total Environ. 656, 39–44. https://doi.org/10.1016/j.scitotenv.2018.11.326.

Yang, N., Hafez, H., Nakhla, G., 2015. Impact of volatile fatty acids on microbial electrolysis cell performance. Bioresour. Technol. 193, 449–455. https://doi.org/10.1016/j.biortech.2015.06.124.

Yu, J., Park, Y., Kim, B., Lee, T., 2015. Power densities and microbial communities of brewery wastewater-fed microbial fuel cells according to the initial substrates. Bioprocess Biosyst. Eng. 38, 85–92. https://doi.org/10.1007/s00449-014-1246-x.

Zhang, J., Chang, H., Li, X., Jiang, B., Wei, T., Sun, X., Liang, D., 2022. Boosting hydrogen production from fermentation effluent of biomass wastes in cylindrical single-chamber microbial electrolysis cell. Environ. Sci. Pollut. Res. 29, 89727–89737. https://doi.org/10.1007/s11356-022-22095-9.

Zhang, Y., Min, B., Huang, L., Angelidaki, I., 2011. Electricity generation and microbial community response to substrate changes in microbial fuel cell. Bioresour. Technol. 102, 1166–1173. https://doi.org/10.1016/j.biortech.2010.09.044.

Zhang, F., Xia, X., Luo, Y., Sun, D., Call, D.F., Logan, B.E., 2013. Improving startup performance with carbon mesh anodes in separator electrode assembly microbial fuel cells. Bioresour. Technol. 133, 74–81. https://doi.org/10.1016/j.biortech.2013.01.036.

Zhuang, K., Vemuri, G.N., Mahadevan, R., 2011. Economics of membrane occupancy and respiro-fermentation. Mol. Syst. Biol. 7, 1–9. https://doi.org/10.1038/msb.2011.34.